

$\pi^+ - \pi^0$ mass difference
from the Bethe-Salpeter equation

Masayasu HARADA*, Masafumi KURACHI† and Koichi YAMAWAKI‡

*Department of Physics, Nagoya University
Nagoya 464-8602, Japan***Abstract**

In the framework of the Schwinger-Dyson equation and the Bethe-Salpeter equation in the improved ladder approximation, we calculate the $\pi^+ - \pi^0$ mass difference on the same footing as the pion decay constant and the QCD S parameter (or L_{10}) through the difference between the vector current correlator Π_{VV} and the axial-vector current correlator Π_{AA} . We find that all the results can be fit to the experimental values for rather large $\Lambda_{\text{QCD}} \sim 700\text{MeV}$ which reflects the “scale ambiguity”. By fitting to the calculated data using the pole saturated form of $\Pi_{VV} - \Pi_{AA}$, we also derive masses and decay constants of ρ meson and a_1 meson, which we found are consistent with the experiments rather insensitively to the “scale ambiguity”.

*harada@eken.phys.nagoya-u.ac.jp

†kurachi@eken.phys.nagoya-u.ac.jp

‡yamawaki@eken.phys.nagoya-u.ac.jp

1 Introduction

The $\pi^+ - \pi^0$ mass difference $\Delta m_\pi^2 \equiv m_{\pi^+}^2 - m_{\pi^0}^2$ is an interesting quantity to measure an explicit breaking of the chiral symmetry by the gauge coupling ($U(1)_{\text{em}}$) in the spontaneously broken phase of the chiral symmetry. It in fact has been a prototype of the mass calculation of pseudo Nambu-Goldstone (NG) bosons in strong coupling gauge theories such as those in the technicolor theories [1] and more recently in the little Higgs models [2]. The sign as well as the absolute value of Δm_π^2 is an important issue (“vacuum alignment problem”), since the negative sign would imply that the vacuum would align so as to break spontaneously the gauge symmetry ($U(1)_{\text{em}}$ in the case of pion) which explicitly breaks the spontaneously broken symmetry. Such a situation never happens in the real-life QCD but may do in other theories. Hence this type of calculation plays a central role of the model buildings.

The first successful calculation of Δm_π^2 [3] was done by the current algebra in conjunction with the Weinberg spectral function sum rules [4] saturated by the π , ρ and a_1 meson poles. Somewhat more elaborate calculation on this line was done combined with the QCD information [5]. Recently, an effective field theory calculation without a_1 meson has been successfully done [6], based on the Hidden Local Symmetry (HLS) model [7, 8, 9] at loop level [10, 11] and the Wilsonian matching [12] of the HLS model with the QCD (for reviews of the HLS approach, see [13, 14]). Ref. [6] demonstrated that the HLS model is a little Higgs model with two sites and two links (open moose) whose locality of theory space forbids quadratic divergence in Δm_π^2 even without a_1 meson.

On the other hand, direct QCD calculation of the Δm_π^2 has never been done except for the lattice simulation [15]. Although the lattice QCD is a powerful method, it is still important to establish alternative QCD-based methods which are more intuitive and less dependent on the power of computers. Such methods will be crucial to the subjects which are difficult to be studied in the framework of the lattice simulation. Most relevant subjects are the dynamical origin of the electroweak symmetry breaking, QCD at finite density, etc.

In this paper, we calculate in the chiral symmetric limit the Δm_π^2 simultaneously with the pion decay constant f_π and the QCD S parameter [16] (or the Gasser-Leutwyler parameter L_{10} [17]) within the framework of the Schwinger-Dyson (SD) equation and the Bethe-Salpeter (BS) equation in the improved ladder approximation. We note that all these quantities are given by “generalized” Weinberg spectral function sum rules for the difference between the vector current correlator Π_{VV} and the axial-vector current correlator Π_{AA} : f_π^2 is given by the Weinberg first sum rule, the S parameter by the Das-Mathur-Okubo (DMO) sum rule [18] or the “zerth Weinberg sum rule”, and Δm_π^2 by the Das-Guralnik-Mathur-Low-Young (DGMLY) sum rule [3] or the “third Weinberg sum rule”. We then rewrite them in terms of the current correlators instead of the spectral functions and directly calculate Δm_π^2 on the same footing as f_π and the QCD S parameter through $\Pi_{VV} - \Pi_{AA}$ in the *space-like momentum region*. Such correlators are written in terms of the BS amplitudes which are given by solving the *inhomogeneous* BS (IBS) equation and the SD equation

with the improved ladder approximation in the Landau gauge both in the *space-like region*. In contrast to our case, solving the bound state spectra by the homogenous BS equation in the time-like region is usually difficult, since it would need analytic continuation of the running coupling which is not an analytic function.¹

This kind of method has been extensively used to investigate masses and decay constants of low lying mesons [20, 21, 22] in good agreement with the experiments. On the other hand, the same method failed to reproduce the QCD S parameter consistently with the experiment [23].

However, we find that the QCD S parameter is rather sensitive to the infrared (IR) cutoff parameter of the QCD running coupling. We actually reproduce the QCD S parameter consistently with the experiment by setting the IR cutoff parameter in the region never investigated in the previous works. Our parameter choice corresponds to taking the QCD scale parameter as $\Lambda_{\text{QCD}} \simeq 724 \text{ MeV}$, while it was chosen as $\Lambda_{\text{QCD}} \simeq 500 \text{ MeV}$ in the previous results of the decay constants and the masses [20, 21] and of the QCD S parameter [23], both values being considerably higher than the conventional $\Lambda_{\text{QCD}}^{(3)} = 300\text{-}450 \text{ MeV}$ obtained in the $\overline{\text{MS}}$ scheme [24]. This actually corresponds to exploiting the “scale ambiguity” [25] of Λ_{QCD} in the SD and BS equations recently emphasized by Hashimoto and Tanabashi [26].

We then show that $\pi^+ - \pi^0$ mass difference Δm_π^2 is calculated in rough agreement with the experimental value for the same parameter region as that reproducing the QCD S parameter and f_π . Actually, although infrared dynamics is quite important for determination of f_π and S , it is not so important for determination of Δm_π^2 . In other words, f_π and S are sensitive to the infrared structure of the running coupling, while Δm_π^2 is not.

We also derive the masses and decay constants of ρ meson and a_1 meson by fitting them to the calculated $\Pi_{VV} - \Pi_{AA}$ within our method using the pole saturated form of $\Pi_{VV} - \Pi_{AA}$. These quantities are also compared with experiments, which is another check of the validity of the calculation in the present analysis.

The calculation presented in this paper turns out to be the first example which derives Δm_π^2 directly from QCD without depending on the lattice simulation. Once we have checked the reliability of such a method in the ordinary QCD (with three light flavors), we may apply it to the mass of pseudo NG bosons and vacuum alignment problem in other strong coupling gauge theories such as the large N_f QCD, walking technicolor, little Higgs, hot/dense QCD, etc..

This paper is organized as follows. In section 2 we introduce spectral function sum rules: The DMO sum rule or the zeroth Weinberg sum rule for S parameter, the first Weinberg sum rule for f_π^2 , the second Weinberg sum rule, and the DGMLY sum rule or the third Weinberg sum rule for Δm_π^2 . We then rewrite them in terms of the current correlators $\Pi_{VV} - \Pi_{AA}$. In section 3 we show how the current correlators are obtained from the BS amplitude which is calculated from the IBS equation in the space-like region. In section 4 we introduce the IBS equation and show how to solve it numerically. Section 5 is the main part of this paper: We first show the result of the

¹See an exception in Ref. [19].

IBS equation for QCD, and discuss the dependence of f_π , S and Δm_π^2 on the infrared structure of the running coupling. Then we compare them with the experimental values. We also show results for masses and decay constants of ρ and a_1 mesons. In section 6 we give summary and discussions on applications to the large N_f QCD and the electroweak symmetry breaking.

2 Spectral function sum rules

In this section we introduce the spectral function sum rules, which express the pion decay constant f_π , the QCD S parameter and Δm_π^2 in terms of $\Pi_{VV} - \Pi_{AA}$ in the space-like momentum region. Here we consider only the chiral symmetric limit of massless three flavors ($N_f = 3$), the corrections of the finite quark mass being expected to be small for the quantities we consider.

Let us begin with introducing the vector and axial-vector currents as

$$V_\mu^a(x) = \bar{\psi}(x)T^a\gamma_\mu\psi(x), \quad (2.1)$$

$$A_\mu^a(x) = \bar{\psi}(x)T^a\gamma_\mu\gamma_5\psi(x), \quad (2.2)$$

where T^a is the generator of $SU(N_f)$ normalized as $\text{tr}(T^aT^b) = \frac{1}{2}\delta^{ab}$ and we consider $a, b = 1, 2, 3$. In the chiral symmetric limit the current correlator Π_{JJ} is given as

$$\delta^{ab} \left(\frac{q_\mu q_\nu}{q^2} - g_{\mu\nu} \right) \Pi_{JJ}(q^2) = i \int d^4x e^{iqx} \langle 0 | T J_\mu^a(x) J_\nu^b(0) | 0 \rangle, \quad (2.3)$$

$$(J_\mu^a(x) = V_\mu^a(x), A_\mu^a(x)).$$

The Umezawa-Kamefuchi-Källén-Lehmann spectral representation for the current correlators are expressed as

$$i \int d^4x e^{iqx} \langle 0 | T J_\mu^a(x) J_\nu^b(0) | 0 \rangle$$

$$= -\delta^{ab} \int_0^\infty ds \frac{1}{s - q^2 - i\epsilon} \left\{ \left(g_{\mu\nu} - \frac{q_\mu q_\nu}{s} \right) \rho_J^{(1)}(s) - q_\mu q_\nu \rho_J^{(0)}(s) \right\}. \quad (2.4)$$

Here, we decomposed the spectral function into the spin-one part $\rho_J^{(1)}(s)$ and spin-zero part $\rho_J^{(0)}(s)$. Since the axial-vector current A_μ^a couples to the massless NG boson, the pion, while no massless particles couple to the vector current V_μ^a , we have

$$\rho_V^{(0)}(s) = 0, \quad (2.5)$$

$$\rho_A^{(0)}(s) = f_\pi^2 \delta(s), \quad (2.6)$$

where f_π is the decay constant of the NG boson π defined by

$$\langle 0 | A_\mu^a(0) | \pi^b(q) \rangle = i q_\mu f_\pi \delta^{ab}. \quad (2.7)$$

Using the spectral functions, we can write down the following “generalized” Weinberg sum rules:

$$\int_0^\infty \frac{ds}{s^2} [\rho_V^{(1)}(s) - \rho_A^{(1)}(s)] = \frac{S}{4\pi}, \quad (2.8)$$

$$\int_0^\infty \frac{ds}{s} [\rho_V^{(1)}(s) - \rho_A^{(1)}(s)] = f_\pi^2, \quad (2.9)$$

$$\int_0^\infty ds [\rho_V^{(1)}(s) - \rho_A^{(1)}(s)] = 0, \quad (2.10)$$

$$-\frac{3\alpha_{em}}{4\pi f_\pi^2} \int_0^\infty ds \log s [\rho_V^{(1)}(s) - \rho_A^{(1)}(s)] = \Delta m_\pi^2, \quad (2.11)$$

where, S is the QCD S parameter [16], which in the case of $N_f = 3$ is related to the Gasser-Leutwyler parameter L_{10} [17] as $S = -16\pi L_{10}$, $\alpha_{em} (= \frac{e^2}{4\pi} = \frac{1}{137})$ is the coupling constant of the electromagnetic interaction, and Δm_π^2 is the $\pi^+ - \pi^0$ mass difference defined by $\Delta m_\pi^2 \equiv m_{\pi^+}^2 - m_{\pi^0}^2$. Equations (2.9) and (2.10) are the first and second Weinberg sum rules [4], respectively, and Eqs. (2.8) is the DMO sum rule [18] or often called the “zeroth Weinberg sum rule”. Equation (2.11) was derived by Das et al. [3] and may be called the DGMLY sum rule or the “third Weinberg sum rule”.

Of course these relations in Eqs. (2.8), (2.9), (2.10), and (2.11) make sense only if the integrals converge. For example, convergence of the second sum rule (2.10) requires that the difference between Π_{VV} and Π_{AA} must satisfy

$$Q^2 [\Pi_{VV}(Q^2) - \Pi_{AA}(Q^2)] \xrightarrow{(Q^2 \rightarrow \infty)} 0, \quad (2.12)$$

where Q^2 is related to the space-like momentum as $Q^2 = -q^2 (> 0)$.

The asymptotic behavior of the current correlators can be calculated by the operator product expansion (OPE) technique. In the chiral limit, the form of $\Pi_{VV}(Q^2) - \Pi_{AA}(Q^2)$ in the ultraviolet region is estimated as follows [27, 28]:

$$\Pi_{VV}(Q^2) - \Pi_{AA}(Q^2) \xrightarrow{(Q^2 \rightarrow \infty)} \frac{4\pi(N_c^2 - 1)}{N_c^2} \frac{\alpha_s \langle \bar{q}q \rangle^2}{Q^4}, \quad (2.13)$$

up to logarithm. This means that $\Pi_{VV}(Q^2) - \Pi_{AA}(Q^2)$ indeed satisfies the condition (2.12) and the relation in Eq. (2.10) makes sense. When the integral in the second sum rule converges, those in the first and zeroth sum rules are also convergent.

Now we rewrite the zeroth and the first sum rules in terms of the current correlators as

$$S = -4\pi \frac{d}{dQ^2} [\Pi_{VV}(Q^2) - \Pi_{AA}(Q^2)] \Big|_{Q^2=0}, \quad (2.14)$$

$$f_\pi^2 = \Pi_{VV}(0) - \Pi_{AA}(0), \quad (2.15)$$

and also the third sum rule: [29]

$$\Delta m_\pi^2 = \frac{3\alpha_{em}}{4\pi f_\pi^2} \int_0^\infty dQ^2 [\Pi_{VV}(Q^2) - \Pi_{AA}(Q^2)]. \quad (2.16)$$

From Eq.(2.16), we can see that the asymptotic behavior (2.13) also guarantees convergence of the third sum rule.

In Ref. [23] the pion decay constant f_π and the QCD S parameter were calculated by the use of the above formulas. However, Δm_π^2 was not calculated so far. So the calculation presented in this paper turns out to be the first example which derives Δm_π^2 directly from QCD without depending on the lattice simulation. Moreover, there is another interest regarding Δm_π^2 related to the structure of the QCD vacuum, as we stressed in the Introduction. When we switch off the electromagnetic interaction and set masses of quarks to be zero, pions are identified with the exact NG bosons associated with the spontaneous breaking of $SU(2)_L \otimes SU(2)_R$ chiral symmetry down to $SU(2)_V$ symmetry. The existence of the electromagnetic interaction explicitly breaks the $SU(2)_L \otimes SU(2)_R$ chiral symmetry, which makes π^+ and π^- be the pseudo NG bosons. On the other hand, π^0 remains massless since the photon does not interact with π^0 . The interesting point here is whether $\Delta m_\pi^2 \equiv m_{\pi^+}^2 - m_{\pi^0}^2$ ($= m_{\pi^+}^2$ in the chiral limit) becomes positive or negative, which is called “vacuum alignment problem”. Negative Δm_π^2 means that fluctuation of π^+ field around $\langle \pi^+ \rangle = 0$ is unstable and the vacuum with $\langle \pi^+ \rangle = 0$ is not a true vacuum. If this is the case, π^+ has non-zero vacuum expectation value and $U(1)_{\text{em}}$ symmetry is broken. We know that, in the real world, Δm_π^2 is positive and the vacuum with $\langle \pi^+ \rangle = 0$ is the true vacuum. $U(1)_{\text{em}}$ symmetry is not broken in the real world. This is quite nontrivial fact resulting from the nonperturbative dynamics of the strong interaction. So it is interesting to investigate whether we can reproduce positive Δm_π^2 which is realized in the real-life QCD.

3 Current correlators from BS amplitudes

In the previous section we have written down the QCD S parameter, f_π , and Δm_π^2 in terms of the current correlators. Then, in this section, we show how the current correlators are obtained from the BS amplitude which will be calculated from the IBS equation.

To derive properties of hadrons as boundstates, it is straightforward to perform calculations directly in the time-like momentum region. However, it is difficult to solve the BS equation and the SD equation in the time-like region since we have to carry out the analytic continuation of the running coupling from the space-like region to the time-like region. In the case of QCD, the one-loop running coupling is not an analytic function, so that we have to approximate it by some analytic function in order to perform the calculations in the time-like region. However, here we need the BS amplitude only for the space-like region in order to calculate the current correlators for Δm_π^2 , f_π and the QCD S parameter.

The BS amplitude $\chi^{(J)}$ ($J = V, A$) is defined in terms of the three-point vertex

function as follows:

$$\delta_i^j \left(\frac{\lambda^a}{2} \right)_f^{f'} \int \frac{d^4 p}{(2\pi)^4} e^{-ipr} \chi_{\alpha\beta}^{(J)}(p; q, \epsilon) = \epsilon^\mu \int d^4 x e^{iqx} \langle 0 | T \psi_{\alpha i f}(r/2) \bar{\psi}_\beta^{j f'}(-r/2) J_\mu^a(x) | 0 \rangle, \quad (3.1)$$

where q^μ is the total momentum of the fermion and anti-fermion and p^μ is the relative one. ϵ^μ is the polarization vector defined by $\epsilon \cdot q = 0$, $\epsilon \cdot \epsilon = -1$, and (f, f') , (i, j) , (α, β) are flavor, color and spinor indices, respectively. Closing the fermion legs of the above three-point vertex function and taking the limit $r \rightarrow 0$, we can express the current correlator in terms of the BS amplitude as follows:

$$\Pi_{JJ}(q^2) = \frac{1}{3} \sum_\epsilon \int \frac{d^4 p}{i(2\pi)^4} \frac{N_c}{2} \text{tr} \left[(\epsilon \cdot G^{(J)}) \chi^{(J)}(p; q, \epsilon) \right] \quad (3.2)$$

where

$$G_\mu^{(V)} = \gamma_\mu, \quad G_\mu^{(A)} = \gamma_\mu \gamma_5, \quad (3.3)$$

and $N_c = 3$ is the number of colors. In the above expression we averaged over the polarizations so that $\Pi_{JJ}(q^2)$ does not depend on the polarization.

We expand the BS amplitude $\chi_{\alpha\beta}^{(J)}(p; q, \epsilon)$ in terms of the bispinor bases $\Gamma_i^{(J)}$ and the invariant amplitudes $\chi_i^{(J)}$ as

$$\left[\chi^{(J)}(p; q, \epsilon) \right]_{\alpha\beta} = \sum_{i=1}^8 \left[\Gamma_i^{(J)}(p; \hat{q}, \epsilon) \right]_{\alpha\beta} \chi_i^{(J)}(p; q), \quad (3.4)$$

where $\hat{q}_\mu = q_\mu / \sqrt{Q^2}$. The bispinor bases can be chosen in a way that they have the same properties of spin, parity and charge conjugation as the corresponding current $J_\mu^a(x)$ has. We adopt the following bispinor bases for the vector vertex:

$$\begin{aligned} \Gamma_1^{(V)} &= \not{\epsilon}, \quad \Gamma_2^{(V)} = \frac{1}{2} [\not{\epsilon}, \not{p}] (p \cdot \hat{q}), \quad \Gamma_3^{(V)} = \frac{1}{2} [\not{\epsilon}, \not{\hat{q}}], \quad \Gamma_4^{(V)} = \frac{1}{3!} [\not{\epsilon}, \not{p}, \not{\hat{q}}] \\ \Gamma_5^{(V)} &= (\epsilon \cdot p), \quad \Gamma_6^{(V)} = \not{p} (\epsilon \cdot p), \quad \Gamma_7^{(V)} = \not{\hat{q}} (p \cdot \hat{q}) (\epsilon \cdot p), \quad \Gamma_8^{(V)} = \frac{1}{2} [\not{p}, \not{\hat{q}}] (\epsilon \cdot p), \end{aligned} \quad (3.5)$$

where $[a, b, c] \equiv a[b, c] + b[c, a] + c[a, b]$. For the axial-vector vertex we use

$$\begin{aligned} \Gamma_1^{(A)} &= \not{\epsilon} \gamma_5, \quad \Gamma_2^{(A)} = \frac{1}{2} [\not{\epsilon}, \not{p}] \gamma_5, \quad \Gamma_3^{(A)} = \frac{1}{2} [\not{\epsilon}, \not{\hat{q}}] (p \cdot \hat{q}) \gamma_5, \\ \Gamma_4^{(A)} &= \frac{1}{3!} [\not{\epsilon}, \not{p}, \not{\hat{q}}] \gamma_5, \quad \Gamma_5^{(A)} = (\epsilon \cdot p) (p \cdot \hat{q}) \gamma_5, \quad \Gamma_6^{(A)} = \not{p} (\epsilon \cdot p) \gamma_5, \\ \Gamma_7^{(A)} &= \not{\hat{q}} (\epsilon \cdot p) (p \cdot \hat{q}) \gamma_5, \quad \Gamma_8^{(A)} = \frac{1}{2} [\not{p}, \not{\hat{q}}] (\epsilon \cdot p) (p \cdot \hat{q}) \gamma_5. \end{aligned} \quad (3.6)$$

From the above choice of the bases, we can easily show that all the invariant amplitudes $\chi_i^{(J)}$ are the even functions of $(p \cdot \hat{q})$ using the charge conjugation property of the current.

In the present analysis we fix the frame of reference in such a way that only the zero component of the total momentum q^μ becomes non-zero. Furthermore, we study

the case where q^μ is in the space-like region. Then, it is convenient to parameterize the total momentum q^μ as

$$q^\mu = (iQ, 0, 0, 0). \quad (3.7)$$

For the relative momentum p^μ , we perform the Wick rotation, and parameterize it by the real variables u and x as

$$p \cdot q = -Q u, \quad p^2 = -u^2 - x^2. \quad (3.8)$$

Consequently, the invariant amplitudes $\chi_i^{(J)}$ become functions in u and x :

$$\chi_i^{(J)} = \chi_i^{(J)}(u, x; Q). \quad (3.9)$$

From the charge conjugation properties for the BS amplitude $\chi^{(J)}$ and the bispinor bases defined above, the invariant amplitudes $\chi_i^{(J)}(u, x)$ are shown to satisfy

$$\chi_i^{(J)}(u, x; Q) = \chi_i^{(J)}(-u, x; Q). \quad (3.10)$$

Using this property of the invariant amplitudes, we rewrite Eq. (3.2) as

$$\Pi_{VV}(Q^2) = \frac{N_c}{\pi^3} \int_0^\infty du \int_0^\infty dx x^2 \left[-\chi_1^{(V)}(u, x; Q) + \frac{x^2}{3} \chi_6^{(V)}(u, x; Q) \right], \quad (3.11)$$

$$\Pi_{AA}(Q^2) = \frac{N_c}{\pi^3} \int_0^\infty du \int_0^\infty dx x^2 \left[\chi_1^{(A)}(u, x; Q) - \frac{x^2}{3} \chi_6^{(A)}(u, x; Q) \right]. \quad (3.12)$$

Here, we used the expanded form of the BS amplitude shown in Eq. (3.4) and carried out the three dimensional angle integration.

From Eqs. (3.11) and (3.12), the quantity $\Pi_{VV} - \Pi_{AA}$ is expressed as

$$\begin{aligned} \Pi_{VV} - \Pi_{AA} &= \frac{1}{3} \sum_\epsilon \int \frac{d^4 p}{i(2\pi)^4} \frac{N_c}{2} \text{tr} \left[\not{\epsilon} \chi^{(J)}(p; q, \epsilon) - \not{\epsilon} \gamma_5 \chi^{(A)}(p; q, \epsilon) \right], \\ &= \frac{N_c}{\pi^3} \int_0^\infty du \int_0^\infty dx x^2 \left[- \left(\chi_1^{(V)}(u, x; Q) + \chi_1^{(A)}(u, x; Q) \right) \right. \\ &\quad \left. + \frac{x^2}{3} \left(\chi_6^{(V)}(u, x; Q) + \chi_6^{(A)}(u, x; Q) \right) \right]. \quad (3.13) \end{aligned}$$

We note that, although either Π_{VV} or Π_{AA} is logarithmically divergent quantity, the difference $\Pi_{VV} - \Pi_{AA}$ becomes finite due to the cancellation of the divergence ensured by the chiral symmetry.

4 Inhomogeneous Bethe-Salpeter equation

In this section we introduce the inhomogeneous Bethe-Salpeter (IBS) equation from which we calculate the BS amplitude defined in the previous section. We also show the numerical method for solving the IBS equation.

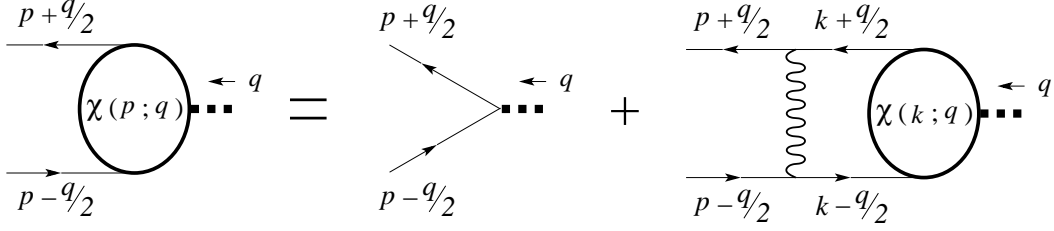


Figure 1: A graphical expression of the IBS equation in the (improved) ladder approximation.

4.1 IBS equation

The IBS equation is the self-consistent equation for the BS amplitude $\chi^{(J)}$, and it is expressed as (see Fig. 1 for graphical expression)

$$T(p; q) \chi^{(J)}(p; q, \epsilon) = \epsilon \cdot G^{(J)} + K(p; k) * \chi^{(J)}(k; q, \epsilon). \quad (4.1)$$

The kinetic part T is given by

$$T(p; q) = S_F^{-1}(p + q/2) \otimes S_F^{-1}(p - q/2), \quad (4.2)$$

where S_F is the full fermion propagator $iS_F^{-1}(p) = \not{p} - \Sigma(p)$. (Note that wave function renormalization factor $A(p)$ becomes unity when we use the Landau gauge.) The BS kernel K in the improved ladder approximation is expressed as

$$K(p; k) = \frac{N_c^2 - 1}{2N_c} \frac{\bar{g}^2(p, k)}{-(p - k)^2} \left(g_{\mu\nu} - \frac{(p - k)_\mu (p - k)_\nu}{(p - k)^2} \right) \cdot \gamma^\mu \otimes \gamma^\nu, \quad (4.3)$$

where $\bar{g}(p, k)$ is the running coupling of QCD whose explicit form will be shown later. In the above expressions we used the tensor product notation

$$(A \otimes B) \chi = A \chi B, \quad (4.4)$$

and the inner product notation

$$K(p; k) * \chi^{(J)}(k; q, \epsilon) = \int \frac{d^4 k}{i(2\pi)^4} K(p, k) \chi(k; q). \quad (4.5)$$

The mass function of the quark propagator is obtained from the SD equation:

$$\Sigma(p) = K(p, k) * iS_F(p). \quad (4.6)$$

It should be stressed that we must use the same kernel $K(p, k)$ as that used in the IBS equation for consistency with the chiral symmetry [30, 31, 32, 33].

4.2 Numerical method for solving the IBS equation

In this subsection we transform the IBS equation in Eq. (4.1) into the form by which we can solve it numerically.

First, we introduce the conjugate bispinor bases defined by

$$\bar{\Gamma}_i^{(J)}(p; q, \epsilon) \equiv \gamma_0 \Gamma_i^{(J)}(p^*; q, \epsilon)^\dagger \gamma_0 . \quad (4.7)$$

Multiplying these conjugate bispinor bases from left, taking the trace of spinor indices and summing over the polarizations, we rewrite Eq. (4.1) into the following form:

$$T_{ij}^{(J)}(u, x) \chi_j^{(J)}(u, x) - \frac{1}{8\pi^3} \int_{-\infty}^{\infty} dv \int_0^{\infty} dy y^2 K_{ij}^{(J)}(u, x; v, y) \chi_j^{(J)}(v, y) = I_i^{(J)}(u, x), \quad (4.8)$$

where the summation over the index j is understood, and

$$I_i^{(J)} = \sum_{\epsilon} \text{tr} \left[\bar{\Gamma}_i^{(J)}(p; q, \epsilon) (\epsilon \cdot G^{(J)}) \right], \quad (4.9)$$

$$T_{ij}^{(J)}(u, x) = \sum_{\epsilon} \text{tr} \left[\bar{\Gamma}_i^{(J)}(p; q, \epsilon) T(p; q) \Gamma_j^{(J)}(p; q, \epsilon) \right], \quad (4.10)$$

$$K_{ij}^{(J)}(u, x; v, y) = \int_{-1}^1 d \cos \theta \sum_{\epsilon} \text{tr} \left[\bar{\Gamma}_i^{(J)}(p; q, \epsilon) K(p, k) \Gamma_j^{(J)}(k; q, \epsilon) \right], \quad (4.11)$$

with the real variables v and y introduced as

$$k \cdot q = -v Q, \quad k \cdot p = -uv - xy \cos \theta. \quad (4.12)$$

Here θ is the angle between the spatial components of p_μ and k_μ .

Using the property of $\chi_i^{(J)}$ in Eq. (3.10), we restrict the integration range as $v > 0$:

$$\int dv K_{ij}(u, x; v, y) \chi_j^{(J)}(v, y) = \int_{v>0} dv [K_{ij}(u, x; v, y) + K_{ij}(u, x; -v, y)] \chi_j^{(J)}(v, y). \quad (4.13)$$

Then, in the following, we treat all the variables u, x, v and y as positive values.

To discretize the variables u, x, v and y we introduce new variables U, X, V and Y as

$$\begin{aligned} u &= e^U, & x &= e^X, \\ v &= e^V, & y &= e^Y, \end{aligned} \quad (4.14)$$

and set ultraviolet (UV) and infrared (IR) cutoffs as

$$U, V \in [\lambda_U, \Lambda_U], \quad X, Y \in [\lambda_X, \Lambda_X]. \quad (4.15)$$

We discretize the variables U and V into $N_{BS,U}$ points evenly, and X and Y into $N_{BS,X}$ points. Then, the original variables are labeled as

$$\begin{aligned} u_{[I_U]} &= \exp[\lambda_U + D_U I_U], & x_{[I_X]} &= \exp[\lambda_X + D_X I_X], \\ v_{[I_V]} &= \exp[\lambda_U + D_U I_V], & y_{[I_Y]} &= \exp[\lambda_X + D_X I_Y], \end{aligned}$$

where $I_U, I_V = 0, 1, 2, \dots (N_{BS,U} - 1)$ and $I_X, I_Y = 0, 1, 2, \dots (N_{BS,X} - 1)$. The measures D_U and D_X are defined as

$$D_U = \frac{\Lambda_U - \lambda_U}{N_{BS,U} - 1}, \quad D_X = \frac{\Lambda_X - \lambda_X}{N_{BS,X} - 1}. \quad (4.16)$$

As a result, the integration is converted into the summation:

$$\int_{v>0} y^2 dy dv \dots \implies D_U D_V \sum_{I_V, I_Y} v y^3 \dots \quad (4.17)$$

In order to avoid integrable singularities in the kernel $K(u, x; v, y)$ at $(u, x) = (v, y)$, we adopt the following four-splitting prescription [21]:

$$K_{ij}(u, x, v, y) \implies \frac{1}{4} [K_{ij}(u, x, v_+, y_+) + K_{ij}(u, x, v_+, y_-) \\ + K_{ij}(u, x, v_-, y_+) + K_{ij}(u, x, v_-, y_-)], \quad (4.18)$$

where

$$v_{\pm} = \exp \left[V \pm \frac{D_U}{4} \right], \quad y_{\pm} = \exp \left[Y \pm \frac{D_X}{4} \right]. \quad (4.19)$$

Now that all the variables have become discrete and the original integral equation (4.1) has turned into a linear algebraic one, we are able to deal it numerically.

5 Results and discussion

In this section, we show the results of calculations and give some discussions. First, we discuss the dependence of the results on the infrared structure of the running coupling. Second, we compare the results with experimental values.

For solving the IBS and SD equations, we have to fix the form of the running coupling $\bar{g}^2(p, k)$ which appears in the IBS and the SD equations. We use the solution of the renormalization group equation for the QCD running coupling with one-loop approximation. We regularize the infrared divergence of the one-loop running coupling by introducing the IR cutoff parameter $t_F (> 0)$ as follows:

$$\alpha(p, k) \equiv \frac{\bar{g}^2(p, k)}{4\pi} = \alpha_0 \frac{1}{\max(t_F, t)}, \quad t = \ln \left[(p_E^2 + k_E^2) / \Lambda_{QCD}^2 \right] \quad (5.1)$$

where $\alpha_0 = 12\pi / (11N_c - 2N_f)$ with N_f being the number of flavors. As for the argument of the running coupling $\bar{g}^2(p, k)$, we used the angle averaged form $p_E^2 + k_E^2$ so that we can analytically carry out the angle integration in the SD and the IBS equations.

In Fig. 2, we plot the solutions of the SD equation for several values of t_F . For smaller value of t_F , the value of mass functions $\Sigma(x)$ in the infrared energy region becomes larger. This is natural because smaller value of t_F means larger running coupling in the infrared region.

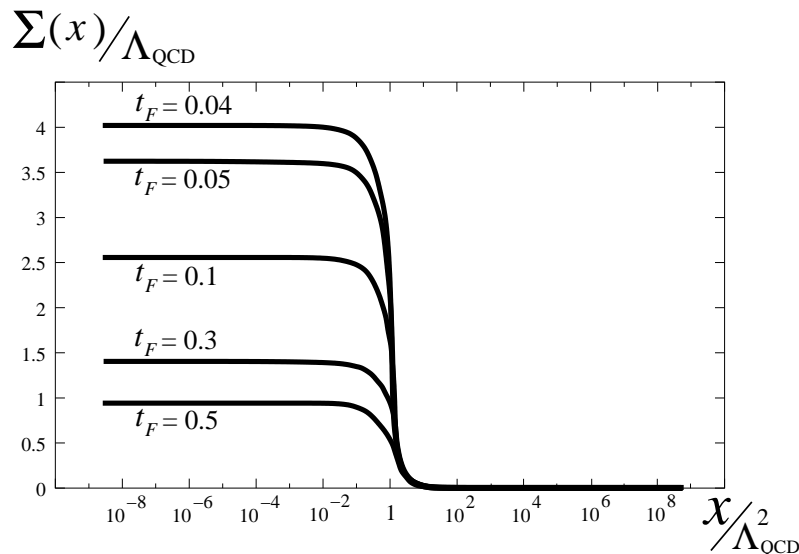


Figure 2: Mass functions obtained from the SD equation for several values of t_F .

When we solve the IBS equation, we use the following parameters:

$$[\lambda_U, \Lambda_U] = [-5.5, 2.5], \quad (5.2)$$

$$[\lambda_X, \Lambda_X] = [-2.5, 2.5], \quad (5.3)$$

$$N_{BS,U} = N_{BS,X} = 30. \quad (5.4)$$

These parameters are chosen so that the dominant supports always lie within the energy region between UV and IR cutoffs for all values of t_F which we use in the present analysis ($t_F = 0.04-0.5$).

5.1 t_F dependence of $\Pi_{VV} - \Pi_{AA}$

In Fig. 3, we plot the resultant values of $\Pi_{VV}(Q^2) - \Pi_{AA}(Q^2)$ for several values of t_F . Horizontal axis shows the square of the Euclidean momentum Q . In this figure, $\Pi_{VV}(Q^2) - \Pi_{AA}(Q^2)$ and Q^2 are normalized by Λ_{QCD}^2 , and plotted as the dimensionless quantities. As we mentioned before, either $\Pi_{VV}(Q^2)$ or $\Pi_{AA}(Q^2)$ is logarithmically divergent. These divergences are expected to be canceled in $\Pi_{VV}(Q^2) - \Pi_{AA}(Q^2)$ ensured by the chiral symmetry. Figure 3 shows this cancellation actually occurs in the present calculation.² From the results shown in Fig. 3, we can see that $\Pi_{VV}(Q^2) - \Pi_{AA}(Q^2)$ is dependent on the value of t_F . In other words, $\Pi_{VV}(Q^2) - \Pi_{AA}(Q^2)$ is sensitive to the infrared structure of the QCD running coupling.

Once we obtain $\Pi_{VV}(Q^2) - \Pi_{AA}(Q^2)$, we can calculate the QCD S parameter, f_π and Δm_π^2 by using Eqs. (2.14), (2.15) and (2.16). In table 1, we list the resultant

²If the quadratic divergences were not canceled, $\Pi_{VV} - \Pi_{AA}$ would become $\frac{\Lambda_{QCD}^2}{8\pi^2} \log \Lambda^2 \sim 0.1\Lambda_{QCD}^2$. Figure 3 shows that $\Pi_{VV} - \Pi_{AA}$ is about $0.03\Lambda_{QCD}^2$ at biggest, so that the divergences are actually canceled with each other.

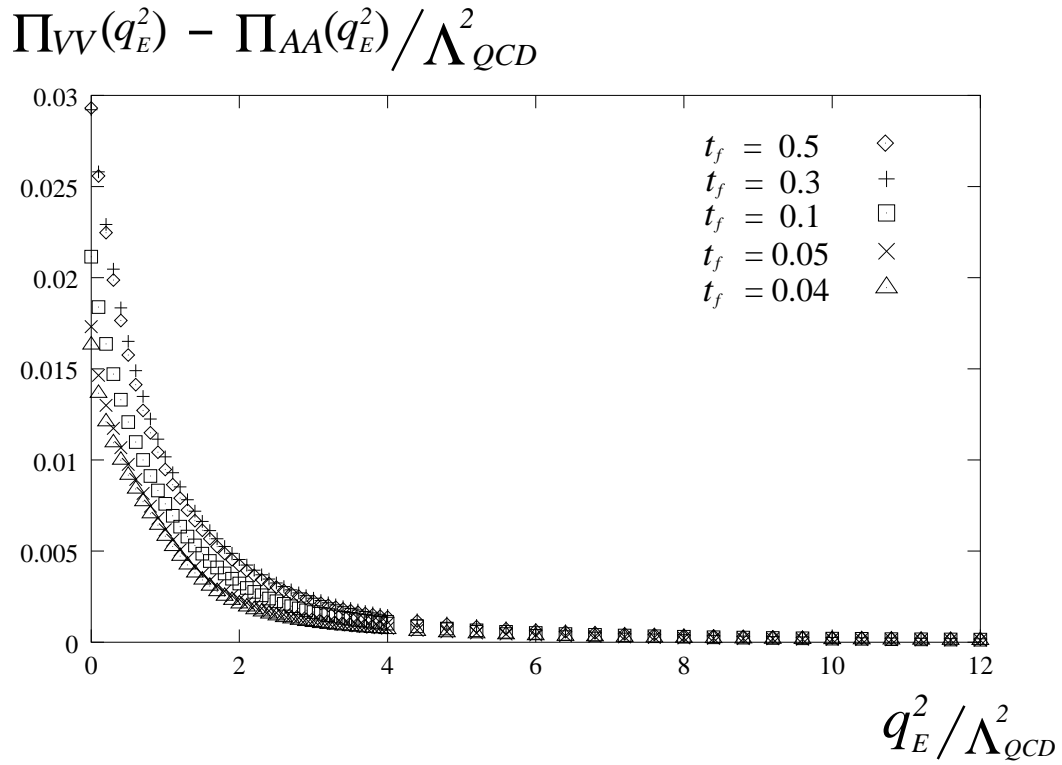


Figure 3: Resultant values of $\Pi_{VV}(Q^2) - \Pi_{AA}(Q^2)$ for several values of t_F . Horizontal axis shows the square of the Euclidean momentum normalized by the scale Λ_{QCD}^2 . $\Pi_{VV}(Q^2) - \Pi_{AA}(Q^2)$ in the vertical axis is also normalized by Λ_{QCD}^2

t_F	0.04	0.05	0.1	0.2	0.3	0.5
S	0.33	0.33	0.35	0.39	0.43	0.47
f_π / Λ_{QCD}	0.128	0.132	0.145	0.162	0.171	0.171
$\Delta m_\pi^2 / \Lambda_{QCD}^2$	0.00201	0.00203	0.00212	0.00215	0.00212	0.00201

Table 1: Resultant values of the QCD S parameter, f_π and Δm_π^2 for several values of t_F . Dimensionfull quantities are normalized by Λ_{QCD} and expressed as dimensionless quantities.

values of these quantities for several values of t_F . Here, we normalized dimensionfull quantities by Λ_{QCD} , and expressed them as dimensionless quantities. These results show that the *QCD S parameter and f_π / Λ_{QCD} are sensitive to the value of IR cutoff parameter t_F while $\Delta m_\pi^2 / \Lambda_{QCD}^2$ is less sensitive to it.* This is natural because the QCD S parameter and f_π are directly related to the infrared quantities as can be easily seen from Eqs. (2.14) and (2.15), while the infrared dependence of the integration of $\Pi_{VV}(Q^2) - \Pi_{AA}(Q^2)$ in Eq. (2.16) is compensated by $f_\pi^2 (= \Pi_{VV}(0) - \Pi_{AA}(0))$ in the denominator.

Table 1 shows that, when we take the value of t_F smaller, the value of f_π / Λ_{QCD} becomes smaller. Here, smaller value of t_F means larger value of infrared running coupling, or, in other words, strong infrared dynamics. At first sight, this behavior seems strange because f_π is the order parameter of the chiral symmetry breaking, and it is expected to reflect the magnitude of the chiral symmetry breaking. One might think that f_π / Λ_{QCD} becomes larger for smaller value of t_F . However, it is not the case. In the present analysis, f_π is not necessarily proportional to the magnitude of the chiral symmetry breaking because QCD with $N_f = 3$ in the vacuum is very far from the chiral phase transition point. To understand this behavior, let us see the Pagels-Stokar (PS) formula [34]³:

$$f_\pi^2 = \frac{N_c}{4\pi^2} \int_0^\infty dx x \frac{\Sigma^2(x) - \frac{x}{4} \frac{d}{dx} [\Sigma^2(x)]}{[x + \Sigma^2(x)]^2}. \quad (5.5)$$

As shown in Fig. 2, the mass functions $\Sigma(x)$ are almost constant for $0 < x = Q^2 < \Lambda_{QCD}^2$ and suddenly drops at $x = \Lambda_{QCD}^2$ for all values of t_F . So we can cut the integration in Eq. (5.5) at $x = \Lambda_{QCD}^2$ and drop the derivative of mass function. We also drop x in the denominator since x satisfies $x \ll \Sigma(x)$ for the relevant integral region ($0 < x < \Lambda_{QCD}^2$). Then we can approximate Eq. (5.5) as

$$f_\pi^2 \simeq \frac{N_c}{4\pi^2} \int_0^{\Lambda_{QCD}^2} dx x \frac{1}{\Sigma^2(0)} \propto \frac{\Lambda_{QCD}^4}{\Sigma^2(0)}. \quad (5.6)$$

From this, we can easily understand that, when infrared dynamics becomes strong, i.e., $\Sigma(0)$ becomes large, f_π becomes small.

³We checked that the difference between f_π calculated from the IBS equation and the PS formula is less than 10 % for all values of t_F . We also checked that qualitative feature of t_F dependence of f_π calculated from the PS formula is not different from f_π obtained from the IBS equation.

t_F	0.04	0.05	0.1	0.2	0.3	0.5	Exp.
Δm_π^2 (MeV ²)	1050	1003	855	698	620	585	1261.1
S	0.33	0.33	0.35	0.39	0.43	0.47	0.32 ± 0.04
f_π (MeV) (input)	92.4	92.4	92.4	92.4	92.4	92.4	92.4

Table 2: Resultant values of Δm_π^2 , S and f_π for several values of t_F . Here, we used $f_\pi = 92.4$ MeV as an input to introduce the physical energy scale. Experimental values of Δm_π^2 and f_π are given in Ref. [35], and S is obtained from the value of the L_{10} given in Ref. [14] through $S = -16\pi \left[L_{10}(\mu) + \frac{1}{192\pi^2} \left(\ln \frac{m_\pi^2}{\mu^2} + 1 \right) \right]$.

For comparison, we consider the decay constant near the chiral phase transition point. In this case, $\Sigma(x)$ becomes very small and Eq. (5.5) is well approximated by

$$f_\pi^2 = \frac{N_c}{4\pi^2} \int_{\Sigma^2(0)}^\infty \frac{dx}{x} \Sigma^2(x). \quad (5.7)$$

From this, we can see that if the running coupling, and then the mass function becomes smaller, f_π also becomes smaller. Thus near the critical point, order parameter f_π is actually proportional to the magnitude of the chiral symmetry breaking. We can actually see this behavior in the large N_f QCD near the critical point (see Figs. 4, 5 in Ref. [19]).

5.2 Comparison with experiments

In this subsection, we compare our results with experiments. So far in this paper, all the dimensionfull quantities were normalized by Λ_{QCD} and dealt as dimensionless quantities. Here, we introduce the “physical energy scale” by setting Λ_{QCD} in a way that it reproduces the experimental value of f_π . Since f_π is sensitive to the infrared parameter, fixing f_π implies that Λ_{QCD} in turn appears sensitive to the infrared parameter and so does the Δm_π^2 which was shown insensitive to the infrared parameter as far as Λ_{QCD} is fixed. We use $f_\pi = 92.4$ MeV as an input to fix Λ_{QCD} in the present analysis.⁴

Table 2 shows comparison of the resultant values of Δm_π^2 and S for several values of t_F with experimental values. Δm_π^2 , S and f_π are directly calculated from $\Pi_{VV}(Q^2) - \Pi_{AA}(Q^2)$ by using Eqs. (2.16), (2.14) and (2.15). From table 2, we can see that if we change the value of t_F , values of Δm_π^2 and S move to opposite directions: When we decrease the value of t_F , Δm_π^2 becomes large, while S becomes small. For the choice $t_F = 0.5$, which was adopted in Ref. [36, 20, 21] as a good regularization in the calculations of the masses and decay constants of ρ and a_1 mesons, we obtained $\Delta m_\pi^2 = 585$ MeV² and $S = 0.47$. Both of these values are far from their experimental values $\Delta m_\pi^2 = 1261.1$ MeV² and $S = 0.29 - 0.36$.

⁴In the chiral symmetry limit of three flavors $m_u = m_d = m_s = 0$, the pion decay constant is estimated as $f_\pi = 86.4 \pm 0.26$ MeV [14]. In this paper we use instead the physical value only for fixing Λ_{QCD} as a reference scale, which is up to the “scale ambiguity” in the SD and BS approach.

However, as we decrease the value of t_F , both Δm_π^2 and S move toward their experimental values. At $t_F = 0.04$, they become

$$\Delta m_\pi^2 = 1050 \text{ MeV}^2, \quad (5.8)$$

$$S = 0.33, \quad (5.9)$$

in good agreement with the experimental value of S and in rough agreement with that of Δm_π^2 . In the case of $t_F = 0.04$ we take

$$\Lambda_{QCD} = 724 \text{ MeV} \quad (5.10)$$

in order to set $f_\pi = 92.4 \text{ MeV}$. This value is much larger than the conventional value of Λ_{QCD} in the $\overline{\text{MS}}$ scheme [24]:

$$\Lambda_{\text{QCD}}^{(3)} = 300 - 450 \text{ MeV}. \quad (5.11)$$

Such a problem already occurred in the previous works [36, 20, 21],

$$\Lambda_{QCD} \simeq 500 \text{ MeV}, \quad (5.12)$$

which roughly corresponds to $t_F = 0.5$ in the present analysis. This reflects the ‘‘scale ambiguity’’ [25], as was recently pointed out in Ref. [26] where an interesting method was proposed to solve it by using the effective coupling.

From these results, we conclude that, when we calculate f_π , Δm_π^2 and S by using the BS equation with the improved ladder approximation, the infrared cutoff parameter t_F should be taken smaller than values used so far in the previous works [36, 20, 21]. This means that the running coupling in the infrared energy region should be taken larger in order to reproduce experimental values of f_π , Δm_π^2 and S at the same time in the calculations based on the BS equation with the improved ladder approximation. (When we take $t_F = 0.04$, the value of the running coupling in the infrared energy region becomes about $\alpha \sim 35$.)

Now let us look at what other quantities can be obtained from $\Pi_{VV} - \Pi_{AA}$. As for ρ meson and a_1 meson, we derive their masses and decay constants by fitting them to the calculated $\Pi_{VV}(Q^2) - \Pi_{AA}(Q^2)$ using the pole saturated form of $\Pi_{VV}(Q^2) - \Pi_{AA}(Q^2)$. Here, we use the following simplest version of the pole saturated form as a fitting function:

$$\left[\Pi_{VV}(Q^2) - \Pi_{AA}(Q^2) \right]_{\text{fit}} = -\frac{Q^2 f_\rho^2}{M_\rho^2 + Q^2} + f_\pi^2 + \frac{Q^2 f_{a_1}^2}{M_{a_1}^2 + Q^2}. \quad (5.13)$$

Resultant best fitted values are listed in table 3 together with the experimental values. From the results shown in this table, we can see that the masses and the decay constants of ρ and a_1 mesons are not so much dependent on the infrared cutoff parameter t_F compared with t_F dependence of Δm_π^2 and S . When we choose $t_F = 0.04$, for which the values of Δm_π^2 and S are predicted in good agreement with experiments,

t_F	0.04	0.05	0.1	0.2	0.3	0.5	Exp.
M_ρ (MeV)	730	710	716	645	613	612	770 - 772
f_ρ (MeV)	150	146	151	150	150	151	154
M_{a_1} (MeV)	1186	1146	1012	908	861	859	1190 - 1270
f_{a_1} (MeV)	115	109	119	118	119	123	144

Table 3: Resultant best fitted values of masses and decay constants of ρ and a_1 mesons for several values of t_F . Experimental values for each quantities are also listed. Experimental values of M_ρ , f_ρ and M_{a_1} are given in Ref. [35], and f_{a_1} is given in Ref. [37].

we obtained

$$M_\rho = 730 \text{ MeV} , \quad (5.14)$$

$$f_\rho = 150 \text{ MeV} , \quad (5.15)$$

$$M_{a_1} = 1186 \text{ MeV} , \quad (5.16)$$

$$f_{a_1} = 115 \text{ MeV} .. \quad (5.17)$$

These are also in good agreement with experiments. This confirms the reliability of calculations in the present analysis based on the improved ladder BS equation with small infrared cutoff parameter ($t_F \sim 0.04$).

6 Summary and Discussions

We have calculated the $\pi^+ - \pi^0$ mass difference Δm_π^2 on the same footing as the pion decay constant f_π and the QCD S parameter through the vector and the axial-vector current correlators. For the calculations we solved inhomogeneous BS equations for the vector and axial-vector vertex functions together with SD equation for the quark mass function within the improved ladder approximation in the Landau gauge. We also obtained the masses and the decay constants of ρ and a_1 mesons by fitting them to $\Pi_{VV}(Q^2) - \Pi_{AA}(Q^2)$ using the pole saturated form.

We showed that all of these quantities are simultaneously fit in agreement with the experiments when we take the IR cutoff parameter $t_F = 0.04$, which corresponds to taking

$$\Lambda_{\text{QCD}} \simeq 724 \text{ MeV} . \quad (6.1)$$

This parameter choice of t_F is fairly smaller than the ones investigated in the previous works [20, 21, 22, 23], which corresponds to

$$\Lambda_{\text{QCD}} \simeq 500 \text{ MeV} . \quad (6.2)$$

Either value of Λ_{QCD} above is substantially larger than that in the $\overline{\text{MS}}$ scheme [24]:

$$\Lambda_{\text{QCD}}^{(3)} = 300 - 450 \text{ MeV} . \quad (6.3)$$

Our results imply that the running coupling of QCD in the IR region should be taken larger than that considered so far, when we calculate not only f_π but also the QCD S

parameter and Δm_π^2 in the framework of the BS and the SD equations in the improved ladder approximation. Apparently, choosing the IR cutoff parameter corresponds to exploiting the “scale ambiguity” [25] of Λ_{QCD} in the SD and BS equations as was recently emphasized in Ref. [26] which proposed an interesting method to resolve the scale ambiguity in the the calculation of f_π .

In order to establish the approach of the SD and the BS equations in the improved ladder approximation, it is certainly desirable to apply the method of Ref. [26] to our case, namely the calculations of Δm_π^2 and QCD S parameter as well as f_π . This will be done in future work.

The success of the analysis based on the BS and the SD equations in the real-life QCD in this paper well motivate us to apply this method for studies of other strong coupling gauge theories. One of the most interesting examples of such is the large N_f QCD (see, e.g., Refs. [38, 39, 40, 41, 42, 43, 19]), which is a QCD with large number of massless flavors (but not too large number as to destroy the asymptotic freedom). It is expected that the chiral symmetry gets restored for a certain large number of massless flavors, which was in fact confirmed by the lattice simulations [41].

It was argued [44, 14] based on the effective field theory of HLS [7, 8, 9] that this chiral restoration of the large N_f QCD is accompanied by the massless vector meson degenerate with the NG boson (pseudoscalar meson) as the chiral partners (“Vector Manifestation” of chiral symmetry). It was further argued [6] that the HLS model even in the real-life QCD behaves as a little Higgs model [2] with two sites and two links, whose locality of theory space forbids the quadratic divergence in Δm_π^2 which is nothing but the (mass)² of the Higgs in the framework of the Little Higgs models. In the large N_f QCD Δm_π^2 becomes small compared with f_π^2 near the chiral restoration point, which may suggest that the large N_f QCD may be considered as a UV completion of the Little Higgs model.

On the other hand, we found in the previous paper [19], by the explicit calculation based on the homogeneous BS and the SD equations in the improved ladder approximation, that masses of the scalar, vector, and axial-vector mesons in the large N_f QCD are proportional to f_π and vanish at the chiral restoration point, which implies somewhat different manifestation than the Vector Manifestation in the HLS model. (This behavior was also conjectured in Ref. [45].)

Thus it would be very useful to clarify the situation to calculate the S parameter and Δm_π^2 in large N_f QCD which have not yet been calculated directly from QCD. In the forthcoming paper we shall calculate Δm_π^2 and S parameter in large N_f QCD by the same method presented in this paper.

Acknowledgments

We would like to thank Yoshio Kikukawa and Masaharu Tanabashi for discussions. M.K. would like to thank Thomas Appelquist for warm hospitality and valuable discussion during his stay at Yale University. This work was supported in part by the JSPS Grant-in-Aid for the Scientific Research (B)(2) 14340072 (K.Y. and M.H.)

and by the 21st Century COE Program of Nagoya University provided by JSPS (15COEG01).

References

- [1] See for reviews, e.g., E. Farhi and L. Susskind, Phys. Rept. **74**, 277 (1981); C. T. Hill and E. H. Simmons, Phys. Rept. **381**, 235 (2003) [Erratum-ibid. **390**, 553 (2004)] and references therein.
- [2] N. Arkani-Hamed, A. G. Cohen and H. Georgi, Phys. Lett. B **513**, 232 (2001) N. Arkani-Hamed, A. G. Cohen, E. Katz, A. E. Nelson, T. Gregoire and J. G. Wacker, JHEP **0208**, 021 (2002) N. Arkani-Hamed, A. G. Cohen, E. Katz and A. E. Nelson, JHEP **0207**, 034 (2002)
- [3] T. Das, G. S. Guralnik, V. S. Mathur, F. E. Low and J. E. Young, Phys. Rev. Lett. **18**, 759 (1967)
- [4] S. Weinberg, Phys. Rev. Lett. **18**, 507 (1967).
- [5] W. A. Bardeen, J. Bijnens and J. M. Gerard, Phys. Rev. Lett. **62**, 1343 (1989).
- [6] M. Harada, M. Tanabashi and K. Yamawaki, Phys. Lett. B **568**, 103 (2003)
- [7] M. Bando, T. Kugo, S. Uehara, K. Yamawaki and T. Yanagida, Phys. Rev. Lett. **54**, 1215 (1985);
- [8] M. Bando, T. Kugo and K. Yamawaki, Nucl. Phys. B **259**, 493 (1985).
- [9] M. Bando, T. Kugo and K. Yamawaki, Prog. Theor. Phys. **73**, 1541 (1985).
- [10] M. Harada and K. Yamawaki, Phys. Lett. B **297**, 151 (1992)
- [11] M. Tanabashi, Phys. Lett. B **316**, 534 (1993)
- [12] M. Harada and K. Yamawaki, Phys. Rev. D **64**, 014023 (2001)
- [13] M. Bando, T. Kugo and K. Yamawaki, Phys. Rept. **164**, 217 (1988).
- [14] M. Harada and K. Yamawaki, Phys. Rept. **381**, 1 (2003)
- [15] A. Duncan, E. Eichten and H. Thacker, Phys. Rev. Lett. **76**, 3894 (1996) A. Duncan, E. Eichten and H. Thacker, Nucl. Phys. Proc. Suppl. **53**, 295 (1997)
- [16] M. E. Peskin and T. Takeuchi, Phys. Rev. Lett. **65**, 964 (1990); Phys. Rev. D **46**, 381 (1992).
- [17] J. Gasser and H. Leutwyler, Annals Phys. **158**, 142 (1984). Nucl. Phys. B **250**, 465 (1985).

- [18] T. Das, V. S. Mathur and S. Okubo, Phys. Rev. Lett. **19**, 859 (1967).
- [19] M. Harada, M. Kurachi and K. Yamawaki, Phys. Rev. D **68**, 076001 (2003)
- [20] K. I. Aoki, M. Bando, T. Kugo, M. G. Mitchard and H. Nakatani, Prog. Theor. Phys. **84**, 683 (1990).
- [21] K. I. Aoki, T. Kugo and M. G. Mitchard, Phys. Lett. B **266**, 467 (1991).
- [22] C. D. Roberts and S. M. Schmidt, Prog. Part. Nucl. Phys. **45**, S1 (2000)
- [23] M. Harada and Y. Yoshida, Phys. Rev. D **50**, 6902 (1994)
- [24] A. J. Buras, arXiv:hep-ph/9806471.
- [25] S. J. Brodsky, G. P. Lepage and P. B. Mackenzie, Phys. Rev. D **28**, 228 (1983).
- [26] M. Hashimoto and M. Tanabashi, arXiv:hep-ph/0210115; M. Hashimoto and M. Tanabashi, in *Proceedings of the 2002 International Workshop on Strong Coupling Gauge Theories and Effective Field Theories (SCGT 02)*, Nagoya, Japan, Dec 10-13, 2002, ed. M. Harada, Y. Kikukawa, and K. Yamawaki (World Scientific Pub. Co., Singapore 2003), p.96-102.
- [27] C. W. Bernard, A. Duncan, J. LoSecco and S. Weinberg, Phys. Rev. D **12**, 792 (1975).
- [28] M. A. Shifman, A. I. Vainshtein and V. I. Zakharov, Nucl. Phys. B **147**, 385 (1979); M. A. Shifman, A. I. Vainshtein and V. I. Zakharov, Nucl. Phys. B **147**, 448 (1979).
- [29] K. Yamawaki, Phys. Lett. B **118**, 145 (1982).
- [30] T. Maskawa and H. Nakajima, Prog. Theor. Phys. **52**, 1326 (1974); T. Maskawa and H. Nakajima, Prog. Theor. Phys. **54**, 860 (1975).
- [31] T. Kugo and M. G. Mitchard, Phys. Lett. B **282**, 162 (1992).
- [32] T. Kugo and M. G. Mitchard, Phys. Lett. B **286**, 355 (1992).
- [33] M. Bando, M. Harada and T. Kugo, Prog. Theor. Phys. **91**, 927 (1994)
- [34] H. Pagels and S. Stokar, Phys. Rev. D **20**, 2947 (1979).
- [35] K. Hagiwara *et al.* [Particle Data Group Collaboration], Phys. Rev. D **66**, 010001 (2002).
- [36] T. Kugo, in *Proc. of 1991 Nagoya Spring School on Dynamical Symmetry Breaking, Nakatsugawa, Japan, 1991*, ed. K. Yamawaki (World Scientific, Singapore, 1992).
- [37] N. Isgur, C. Morningstar and C. Reader, Phys. Rev. D **39**, 1357 (1989).

- [38] T. Banks and A. Zaks, Nucl. Phys. B **196**, 189 (1982).
- [39] T. Appelquist, J. Terning and L. C. Wijewardhana, Phys. Rev. Lett. **77**, 1214 (1996) T. Appelquist, A. Ratnaweera, J. Terning and L. C. Wijewardhana, Phys. Rev. D **58**, 105017 (1998)
- [40] V. A. Miransky and K. Yamawaki, Phys. Rev. D **55**, 5051 (1997) [Erratum-ibid. D **56**, 3768 (1997)]
- [41] J. B. Kogut and D. K. Sinclair, Nucl. Phys. B **295**, 465 (1988); F. R. Brown, H. Chen, N. H. Christ, Z. Dong, R. D. Mawhinney, W. Schaffer and A. Vaccarino, Phys. Rev. D **46**, 5655 (1992); Y. Iwasaki, K. Kanaya, S. Sakai and T. Yoshie, Phys. Rev. Lett. **69**, 21 (1992); Y. Iwasaki, K. Kanaya, S. Kaya, S. Sakai and T. Yoshie, Nucl. Phys. Proc. Suppl. **53**, 449 (1997); Prog. Theor. Phys. Suppl. **131**, 415 (1998).
- [42] R. Oehme and W. Zimmermann, Phys. Rev. D **21**, 471 (1980).
- [43] M. Velkovsky and E. Shuryak, Phys. Lett. B **437**, 398 (1998).
- [44] M. Harada and K. Yamawaki, Phys. Rev. Lett. **86**, 757 (2001)
- [45] R. S. Chivukula, Phys. Rev. D **55**, 5238 (1997)